

Solvable optimal velocity models and asymptotic trajectory

Ken Nakanishi*

Department of Physics, Kyoto University, Kyoto 606-01, Japan

Katsumi Itoh[†] and Yuji Igarashi[‡]

Physics Division, Department of Education, Niigata University, Niigata 950-21, Japan

Masako Bando[§]

Physics Division, Aichi University, Miyoshi, Aichi 470-02, Japan

(Received 23 October 1996)

In the optimal velocity model proposed as a version of car following model, it has been found that a congested flow is generated spontaneously from a homogeneous flow for a certain range of the traffic density. A well-established congested flow obtained in a numerical simulation shows a remarkable repetitive property, such that the velocity of a vehicle evolves exactly in the same way as that of its preceding one except with a time delay T . This leads to a global pattern formation in time development of the vehicle's motion, and gives rise to a closed trajectory on Δx - v (headway-velocity) plane connecting congested and free flow points. To obtain the closed trajectory analytically, we propose an approach to the pattern formation, which makes it possible to reduce the coupled car following equations to a single difference-differential equation (Rondo equation). To demonstrate our approach, we employ a class of linear models which are exactly solvable. We also introduce the concept of "asymptotic trajectory" to determine T and v_B (the backward velocity of the pattern), the global parameters associated with the vehicle's collective motion in a congested flow, in terms of parameters, such as the sensitivity a , which appeared in the original coupled equations. [S1063-651X(97)13105-1]

PACS number(s): 64.60.Lx, 89.40.+k, 02.30.Ks, 02.60.Cb

I. INTRODUCTION

Traffic flow is one of the most interesting phenomena of many-body systems which may be controlled by a basic dynamical equation. Recent developments in the study of traffic flow has brought a renewed interest in microscopic approaches, such as the optimal velocity model (OV model) [1–3], which is a new version of the car following model [4–6], cellular automaton models [7–9], coupled map lattice models [10], and the fluid dynamical models [11]. The OV-model, among others, has especially attracted interest because it provides us with a possibility of unified understanding of both free and congested traffic flows from common basic dynamical equations. Unlike traditional car following models, it introduces optimal velocity function $V(\Delta x)$ as a desirable velocity depending on headway distance Δx . The basic equation of the OV model for a series of vehicles on a circuit of length L is

$$\ddot{x}_n(t) = a\{V[\Delta x_n(t)] - \dot{x}_n(t)\} \quad n = 1, 2, \dots, N, \quad (1.1)$$

where x_n denotes the position of the n th vehicle, $\Delta x_n \equiv x_n - x_{n-1}$ headway, and N the total vehicle number. The constant parameter a is the sensitivity. A driver accelerates (or decelerates) his vehicle in proportion to the differ-

ence between his velocity and the optimal velocity $V(\Delta x)$. As easily noticed, a homogeneous flow is a solution to Eq. (1.1). In such a flow, vehicles have a common headway L/N , which is the inverse of the vehicle density. Stability of homogeneous flows is analyzed within a linear approximation [1,2]; it is stable for $f = V'(L/N) < f_c$ and unstable for $f > f_c$. The critical value is found to be $f_c = a/2$.

In order to demonstrate that the OV model describes "spontaneous generation of congestion," numerical simulations were made using Eq. (1.1). It was found that for $f < f_c$, i.e., if the density is above the critical value, a slightly perturbed homogeneous flow develops to a congested flow after enough time. The congested flow consists of alternating two distinct regions; congested regions (high density), and smoothly moving regions or free regions (low density). In this way the traffic congestion occurs spontaneously in the OV model. This phenomenon can be understood as a sort of phase transition from a homogeneous flow state to a congested flow state [1,2].

A remarkable feature of the well-established congested flow is that the velocity of the n th vehicle \dot{x}_n has the same time dependence as that of the preceding $[(n-1)$ th] vehicle, except at a certain time delay T . It is also found that the global pattern moves backward with a velocity v_B . This kind of behavior of the vehicles may be called "repetitive pattern formation." It leads to formation of a closed trajectory ("limit cycle") on an Δx - v plane, along which representative points for all the vehicles move one after another. The convergence of the vehicle's trajectories to a closed trajectory signals the congestion in a traffic flow. Therefore, the determination of the closed trajectory is one of the most im-

*Electronic address: nakanisi@gauge.scphys.kyoto-u.ac.jp

[†]Electronic address: itoh@ed.niigata-u.ac.jp

[‡]Electronic address: igarashi@ed.niigata-u.ac.jp

[§]Electronic address: bando@aichi-u.ac.jp

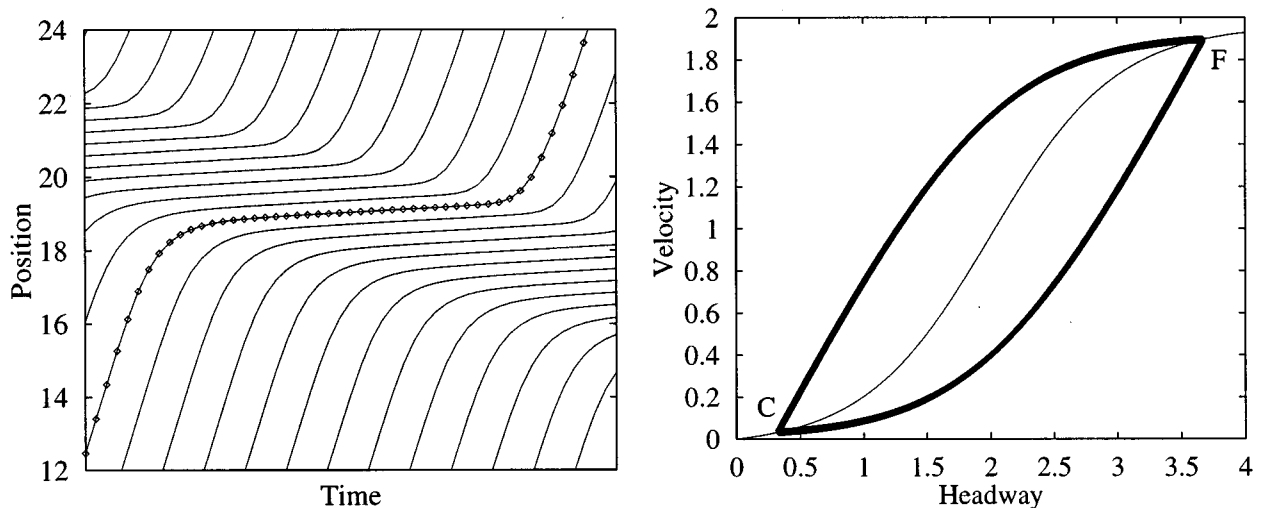


FIG. 1. A result of the numerical simulation with 20 vehicles on a circuit with the circumference $L=40$. The sensitivity and the OV function are chosen as $a=1.0$ and $V(h)=\tanh(h-2)+\tanh(2)$. (a) Trajectories of vehicles passing through a congested region. (b) The “limit cycle” on the Δx - v (headway-velocity) plane. The cusp points C and F correspond to congested and free regions, respectively. Representative points for vehicles move anticlockwise along this “limit cycle.” They run fast on curves connecting the two cusps, while they stay around cusps for a while. The thin line shows the OV function.

portant subjects to understand congested flows. However this has been done mostly in computer simulations. The purpose of the present paper is to obtain this closed trajectory directly by an analytical method. Actually it has been found that, in the vicinity of the critical point for the congested flow, Eq. (1.1) can be reduced to the modified Korteweg-de Vries equation by the dynamical reduction method [12]. In this paper we propose an analytical approach to the pattern formation, which may be applicable to any congested flow.

We argue that, once the repetitive pattern is formed, the coupled car following equations reduce to a single difference-differential equation (Rondo equation) for a universal function (Rondo function). A Rondo function determines a closed trajectory on an Δx - v plane. To make the Rondo equation tractable, we have simplified our question on the following two points: firstly, we have assumed that OV functions are piecewise linear; secondly, we have concentrated our attention on an asymptotic trajectory, which is the key concept to be explained in Sec. II. We would like to stress that our method does not lose its generality by making the above assumption on OV functions: an OV function to be obtained from real data may be approximated by a piecewise linear function.

With the above simplifications, we have solved the Rondo equation for each model and given an asymptotic trajectory on the Δx - v plane. Our result clearly tells us that, once an OV function and the sensitivity a are given, an asymptotic trajectory is uniquely determined; this then implies that the parameters T and v_B for a collective motion of vehicles are given as a function of a . Therefore, our approach provides us with a method to determine a dependence of the global parameters T and v_B .

This paper is organized as follows. Section II summarizes the main results obtained from numerical simulations of the OV model, with emphasis on the pattern formation in a congested flow. The concept of an asymptotic trajectory is explained in Sec. II. As will become clear in later sections, an asymptotic trajectory is a very important concept for under-

standing the OV model. We derive the difference-differential equation and present a general strategy on how to solve it in Sec. III. This part summarizes the central idea of this paper. In order to demonstrate how the Rondo approach works, we analytically solve, in Sec. IV, some simple models with piecewise linear OV functions. Our first model has been investigated by Sugiyama and Yamada [13]. Here we solve this model in the context of the Rondo approach. Although an asymptotic trajectory is very close to a real trajectory observed in a computer simulation, it is not exactly the same as the latter. We describe some aspects of real trajectories based on our knowledge of the asymptotic one in Sec. V. Section VI is devoted to summary and discussions.

II. PATTERN FORMATION IN OV MODEL

Let us recollect what we have learned with the numerical simulations of an OV model [1–3]. Suppose a simulation is performed with a given OV function and a fixed sensitivity a . After a congested flow is well established, typical features of the repetitive behavior can be observed in the following two figures.

Figures 1(a) and 1(b) show that vehicles move in alternating regions of free and congested flows. It is recognized that every vehicle behaves in the same manner as its preceding one with a certain time delay T : as a result, the congested region moves backward with the velocity v_B . Once the location of any vehicle, say, the n th vehicle, is given as a function of t , we may reproduce the pattern in Fig. 1(a) by plotting a series of functions shifted in time and position by T and $v_B T$ appropriately. Therefore, we expect that a congested flow may be completely determined by a function of t and global parameters T and $v_B T$. The precise specifications of our approach to this repetitive behavior will be explained in Sec. III.

Figure 1(b) clearly shows there exists a “limit cycle” on the Δx - v plane, a closed curve with two cusps at points $C(\Delta x_C, v_C)$ and $F(\Delta x_F, v_F)$, both of which are on the OV

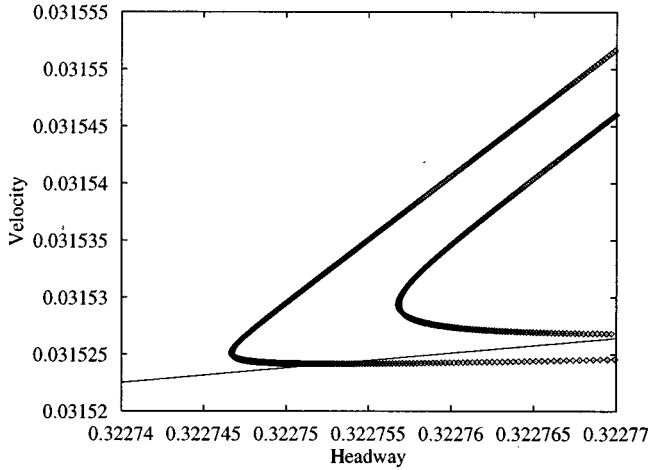


FIG. 2. Trajectories for a vehicle passing through two congested regions different in size. The outer curve corresponds to the larger congested region. The thin line is the OV function. Parameters are the same as those in Fig. 1.

function. At these cusp points, we find $V'(\Delta x) < a/2$, which means that homogeneous flows with such headways and velocities are linearly stable. Representative points for all vehicles move on this ‘‘limit cycle’’ in an anticlockwise direction. It follows from the conservation of flow

$$\frac{v_C + v_B}{\Delta x_C} = \frac{v_F + v_B}{\Delta x_F} = \frac{1}{T}, \quad (2.1)$$

that the straight line connecting C and F has the slope T^{-1} and intersects with the vertical axis at $-v_B$. (This relation is an approximate one except for an asymptotic trajectory to be discussed below.)

In the rest of this section, we would like to explain the concept of an asymptotic trajectory on the Δx - v plane. Suppose that a vehicle passes through two congested regions different in size on a circuit. Then the representative point moves on curves as shown in Fig. 2. Each trajectory may not form an actual cusp, rather it will form a round shaped tip. Also we find that the larger the congested region, the sharper the shape of the tip: the minimum velocity of the vehicle is smaller for a longer congestion. It is rather easy to imagine that for a very short congestion the vehicle cannot decelerate itself enough to reach the velocity appropriate for a longer congested region. If we plot minimum velocities for longer and longer congested regions, we would find a limiting value for the minimum velocities. This value must be realized for an infinitely long congested region. With a similar argument we find the limiting value for maximum velocities corresponding to an infinitely long free region. We may imagine the following extreme situation: a vehicle starting from an infinitely long free (congested) region goes toward an infinitely long congested (free) region. The trajectory for this limiting situation will be called a decelerating (an accelerating) asymptotic trajectory. Combining them we would find a closed curve with two real cusps on the OV function.

The duration for a vehicle to stay in a congested region would obviously get longer for a larger congested region. For an asymptotic trajectory it becomes infinite. This does fit to our linear analysis since the behavior of a vehicle is con-

trolled by exponential functions in time. In Sec. V, we shall see that exponential functions determine a curve near a cusp.

III. RONDO APPROACH

We begin our description of the Rondo approach with two basic assumptions.

(1) Velocities of the n th and $(n-1)$ th vehicles have exactly the same time dependence if a certain time delay T is taken into account, $\dot{x}_{n-1}(t) = \dot{x}_n(t+T)$.

(2) The pattern of traffic flow moves backward with a constant velocity v_B .

The above described properties are expressed as,

$$x_{n-1}(t) = x_n(t+T) + v_B T. \quad (3.1)$$

All the vehicle’s behavior is represented with a single universal function $F(t) \equiv x_n(t)$ (this assumption bears some similarities with the traveling wave ansatz [$\phi(x,t) \rightarrow f(x-vt)$] for the wave equation),

$$x_{n-k}(t) = F(t+kT) + kv_B T. \quad (3.2)$$

With the n th vehicle’s headway given as

$$\Delta x_n(t) = F(t+T) - F(t) + v_B T, \quad (3.3)$$

the N coupled car following Eq. (1.1) is reduced to a single difference-differential equation for $F(t)$,

$$\frac{1}{a} \ddot{F}(t) + \dot{F}(t) = V[F(t+T) - F(t) + v_B T]. \quad (3.4)$$

In the following it will be called the Rondo equation.

In this paper, we will seek the Rondo function $F(t)$ for the asymptotic trajectory (we will discuss more realistic situations with finite congested regions in Sec. V). Before studying concrete models, let us consider its generic properties. Since the position and the velocity of vehicles are obviously continuous in time, $F(t)$ is a continuously differentiable function.

An asymptotic trajectory connects the points F and C , each of which corresponds to an infinitely long free or congested region (an approximately homogeneous flow) satisfying the stability condition mentioned in Sec. II. Therefore $F(t)$ should be homogeneous flows asymptotically in the infinite past and future: $\dot{F}(t) \rightarrow \text{const}$ as $t \rightarrow \pm\infty$. An asymptotic trajectory interpolates two stable solutions of Eq. (1.1). In this sense $F(t)$ may be regarded as a ‘‘kink solution.’’

Like OV models studied in earlier papers, each model in Sec. IV has an OV function which is symmetric with respect to a point, $S(\Delta x_S, v_S)$ (the symmetry of an OV function is absolutely not necessary to solve a system in the Rondo approach. In Sec. VI, we discuss how to solve the Rondo equation for a generic situation). So we assume this property in the following arguments and quote our result in Appendix A. Two end points of an asymptotic trajectory, $C(\Delta x_C, v_C)$ and $F(\Delta x_F, v_F)$, are symmetric with respect to S . Three points C , F , and S are on a straight line with a slope T^{-1} and an

intersection $-v_B$. Note that once the slope is given, the intersection is uniquely determined since point S must be on the line.

As shown in Appendix A, accelerating and decelerating asymptotic trajectories are symmetric with respect to S . Therefore it is sufficient to study one of them; in the rest of this paper, we will take a decelerating asymptotic trajectory. Here we summarize conditions which should be satisfied by the function $F(t)$: (1) $F(t)$ and $\dot{F}(t)$ are continuous for any $t(F(t) \in C^1)$; (2) $v_F = \lim_{t \rightarrow -\infty} \dot{F}(t)$ and $v_C = \lim_{t \rightarrow +\infty} \dot{F}(t)$; (3) $v_F + v_C = 2v_S$ and $\Delta x_F + \Delta x_C = 2\Delta x_S$, where $\Delta x_F = \lim_{t \rightarrow -\infty} [F(t+T) - F(t) + v_B T]$ and $\Delta x_C = \lim_{t \rightarrow +\infty} [F(t+T) - F(t) + v_B T]$.

We would like to explain a way to solve the Rondo equation, which contains an OV function and a sensitivity a , as well as T and v_B associated the pattern formation. (1) First we give the parameter T . By drawing a straight line through the point S with the slope T^{-1} , we find the intersection $-v_B$ and the points C and F . (2) Now a is the only free parameter of the Rondo equation. If we could solve the equation, we would obtain a one-parameter family of (or a -dependent) Rondo functions. (3) Among this family, the right Rondo function is selected by requiring that it connects the points C and F . This condition also determines a unique value for a . Accordingly we find the a dependence of T .

IV. PIECEWISE LINEAR FUNCTION MODELS

We consider here a class of models with piecewise linear OV functions. The Rondo equation is now linearized for all regions of Δx , and therefore exactly solvable.

A. Step function model

The first model has the step function for the OV function,

$$V(\Delta x) = \begin{cases} 0 & \Delta x < \Delta x_S \quad (\text{region I}) \\ V_0 & \Delta x > \Delta x_S \quad (\text{region II}). \end{cases} \quad (4.1)$$

This OV model has been solved in Ref. [13]. Here we explain how this model can be solved in our Rondo approach. In this model, the Rondo equation is given by

$$\frac{1}{a} \ddot{F}(t) + \dot{F}(t) = V_0 \theta(F(t+T) - F(t) + v_B T - \Delta x_S), \quad (4.2)$$

where $\theta(x)$ is the Heaviside function.

In the motion corresponding to a decelerating asymptotic trajectory, the representative point for a vehicle moves from region II into region I. Let us take the time t such that the point moves into the region I at $t=0$, which implies $\Delta x_n(0) = \Delta x_S$.

The equation of motion is

$$\frac{1}{a} \ddot{F}(t) + \dot{F}(t) = \begin{cases} V_0 & (t < 0) \\ 0 & (t > 0). \end{cases} \quad (4.3)$$

The general solutions for two regions are

$$\dot{F}(t) = \begin{cases} V_0 + C_1 e^{-at} & (t \leq 0) \\ C_2 e^{-at} & (t \geq 0). \end{cases} \quad (4.4)$$

The integration constants are determined as $C_1=0$ and $C_2=V_0$ from requirements that $\dot{F}(t)$ be a continuous function and asymptotically constant for $t \rightarrow \pm \infty$. The continuous function $F(t)$ is

$$F(t) = \begin{cases} V_0 t & (t \leq 0) \\ \frac{V_0}{a} (1 - e^{-at}) & (t \geq 0). \end{cases} \quad (4.5)$$

Here we choose the origin of position coordinate so that $F(0)=0$.

The function $F(t)$, with its relation to the headway $\Delta x_n(t) = F(t+T) - F(t) + v_B T$, completely determines a decelerating asymptotic trajectory on the Δx - v plane. From condition (3) in Sec. III, the asymptotic trajectory connects symmetric points on the OV function. This gives us a condition $\Delta x_n(+\infty) + \Delta x_n(-\infty) = 2\Delta x_S = 2\Delta x_n(0)$,

$$v_B T + (V_0 + v_B)T = 2 \left[\frac{V_0}{a} (1 - e^{-aT}) + v_B T \right]. \quad (4.6)$$

This may be expressed as the transcendental equation for $\rho = aT$

$$e^{-\rho} + \frac{1}{2}\rho - 1 = 0. \quad (4.7)$$

Since the ρ is found to be the constant (1.593 62...), we obtain

$$aT = \rho = 1.593\ 62\ \dots \quad (4.8)$$

This gives us the a dependence of T , which was first obtained in Ref. [13].

It is instructive to see a relation between the function $F(t)$ and the decelerating trajectory depicted in Fig. 3. Two curves in Fig. 3(b) correspond to the $(n-1)$ th and n th vehicle's locations. At $t=0$ the n th vehicle's representative point moves into region I and $F(t)$ is described by an exponential function. Before that time, the function $F(t)$ is linear in t . The curve for the $(n-1)$ th vehicle changes from the linear to the exponential behavior at $t=-T$. It is given via a parallel displacement by the vector $(-T, v_B T)$ from the curve $F(t)$. For the time $t \leq -T$, curves are two parallel straight lines, which implies the headway of the n th vehicle does not change till that time from the infinite past. The n th vehicle has the constant velocity V_0 for $t < 0$. This tells us that the n th vehicle is in the free region for $t \leq -T$, indicated by the point F in Fig. 3(a). It is also easy to observe that at $t=-T$ the $(n-1)$ th vehicle starts to decelerate. As a result the headway of the n th vehicle decreases; at $t=0$ it reaches the value Δx_S and the n th vehicle starts to decelerate itself.

In this model, the points F and C are both characterized as points which are reached in the infinite future or past. As a traffic flow, we are describing a solitonlike solution connecting half infinite vehicles, running with the velocity v_F and the headway Δx_F , and another half infinite vehicles going into the congested region associated with the point C .

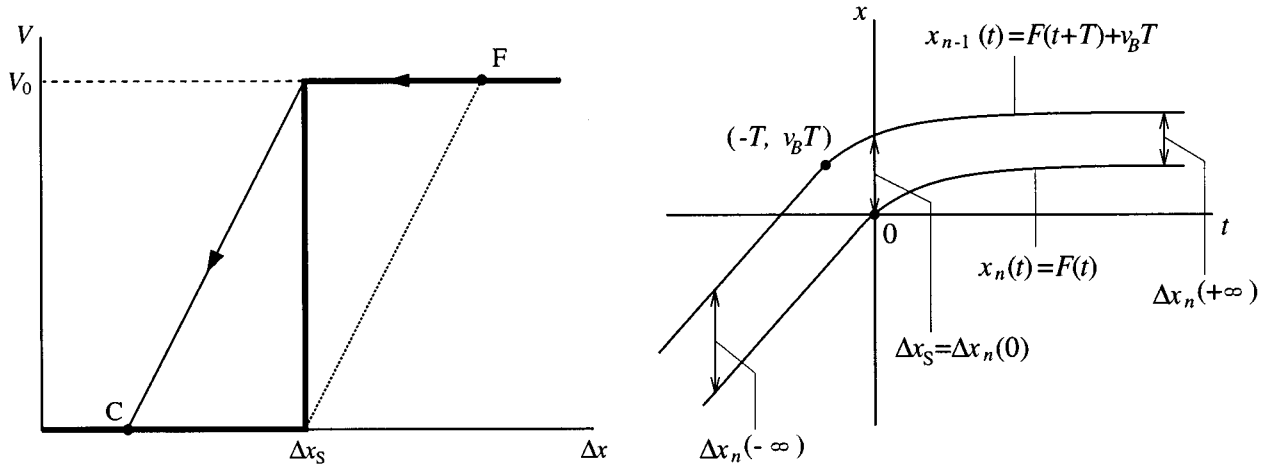


FIG. 3. (a) The OV function (thick line) and a decelerating asymptotic trajectory (thin line with arrows) for the step function model. (b) The position functions $x_n(t)$ and $x_{n-1}(t)$ for the decelerating asymptotic trajectory.

B. Single slope function model

In the step function model, the Δx dependence of the Rondo equation is too simple; T dependence is not explicit. So we would like to consider a slightly improved model, whose OV function shown in Fig. 4 has a finite slope. Thus we call this model the single slope function model. The OV function is characterized by the following parameters: f the slope; V_0 the maximum velocity; Δx_S the headway for optimal velocity $V_0/2$. From the linear analysis in [1], we know that a homogeneous flow becomes unstable and a congested flow is expected for $2f > a$. This condition is assumed in our analysis here.

The OV function has sharp bends at

$$\Delta x_A = \Delta x_S - \frac{V_0}{2f}, \quad (4.9)$$

$$\Delta x_B = \Delta x_S + \frac{V_0}{2f}, \quad (4.10)$$

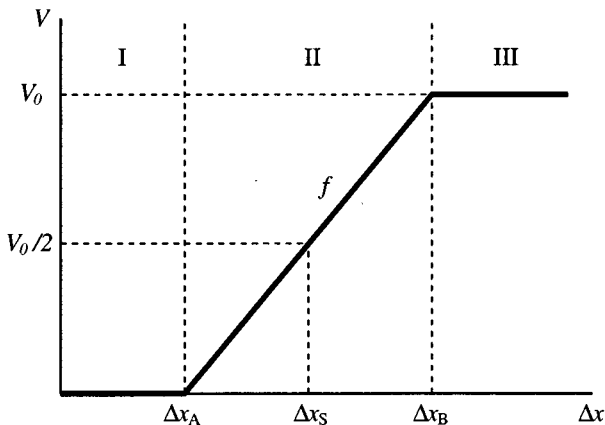


FIG. 4. The OV function for the single slope function model. f is the gradient in region II. The function is symmetric with respect to the point $(\Delta x_S, V_0/2)$.

which divide Δx into three regions, I, II, and III, as indicated in Fig. 4.

We would like to find a Rondo function $F(t)$ for a decelerating asymptotic trajectory, along which headway of a vehicle monotonically decreases from Δx_F to Δx_C . We assume it reaches Δx_B at $t = -\tau$ and Δx_A at $t = 0$. The Rondo equation takes the form

$$\frac{1}{a} \ddot{F}(t) + \dot{F}(t) = \begin{cases} 0 & (t \geq 0) \\ f(F(t+T) - F(t) - \delta) & (-\tau \leq t \leq 0), \\ V_0 & (t \leq -\tau) \end{cases} \quad (4.11)$$

subject to the conditions,

$$F(T) - F(0) + v_B T = \Delta x_A, \quad (4.12)$$

$$F(-\tau + T) - F(-\tau) + v_B T = \Delta x_B. \quad (4.13)$$

Here $\delta = \Delta x_A - v_B T$. Note that the time $-\tau$ is not a free parameter. Rather, it should be determined from Eq. (4.13) via solving the Rondo equation.

For regions I and III, the Rondo equation becomes the same as that in the step function model. Therefore, we obtain

$$\dot{F}(t) = \begin{cases} \text{const} \times e^{-at} & (\text{for region I}) \\ V_0 & (\text{for region III}). \end{cases} \quad (4.14)$$

Our purpose in this subsection is to describe a method to find the Rondo function in region II which correctly interpolates those in Eq. (4.14). To this end, we may introduce a series of functions for each time interval

$$F(t) = \begin{cases} F^I(t) & (0 \leq t) \\ F_1(t) & (-T \leq t \leq 0) \\ F_2(t) & (-2T \leq t \leq -T) \\ \vdots & \vdots \\ F^{III}(t) & (t \leq -\tau). \end{cases} \quad (4.15)$$

The first function $F^I(t) \equiv F_0(t)$ and the last one $F^{III}(t)$ are for regions I and III, respectively.

Let us find $F^I(t)$ (for $t \geq 0$). It follows from Eq. (4.14) that

$$\dot{F}^I(t) = u_0 e^{-at}, \quad (4.16)$$

$$F^I(t) = \frac{u_0}{a} (1 - e^{-at}), \quad (4.17)$$

where we fix again $F^I(0) = 0$. The n th vehicle's headway is then given by

$$\Delta x_n(t) = F^I(t+T) + v_B T - F^I(t) = \frac{u_0}{a} (1 - e^{-aT}) e^{-at} + v_B T. \quad (4.18)$$

Since the condition (4.12) determines the constant u_0

$$u_0 = a \frac{\Delta x_A - v_B T}{1 - e^{-aT}} \equiv \frac{a \delta}{1 - e^{-aT}}, \quad (4.19)$$

we find the Rondo function for $t \geq 0$ to be

$$F^I(t) = \frac{\delta}{1 - e^{-aT}} (1 - e^{-at}). \quad (4.20)$$

This leads to a linear relation between the velocity and the headway

$$\dot{x}_n = \frac{a}{1 - e^{-aT}} (\Delta x_n - v_B T). \quad (4.21)$$

In the $t \rightarrow \infty$ limit, we find that $\dot{x}_n \rightarrow 0$ and $\Delta x_n \rightarrow v_B T$.

Now we consider $F_1(t)$ (for $-T \leq t \leq 0$). In this time interval, the Rondo equation for $F_1(t)$ is expressed as

$$\frac{1}{a} \ddot{F}_1(t) + \dot{F}_1(t) = f(F_0(t+T) - F_1(t) - \delta), \quad (4.22)$$

in terms of the Rondo function for the region I $F^I(t) \equiv F_0(t)$. By using the differential operator

$$\mathcal{D} = \frac{1}{af} \frac{d^2}{dt^2} + \frac{1}{f} \frac{d}{dt} + 1, \quad (4.23)$$

we may rewrite the above equation as

$$\mathcal{D}F_1(t) = F_0(t+T) - \delta. \quad (4.24)$$

The general solution may be written as a sum of a particular solution and the solution to the homogeneous equation $\mathcal{D}F_1^{\text{hom}}(t) = 0$. It is easy to see that $F_0(t+T) - \delta$ is a particular solution, since the function $F_0(t) \equiv F^I(t)$ given in Eq. (4.20) satisfies

$$\mathcal{D}F_0(t) = F_0(t). \quad (4.25)$$

The exponents γ for a homogeneous solution are

$$\gamma = -\frac{a}{2} \pm i \left(af - \frac{a^2}{4} \right)^{1/2} \equiv -\frac{a}{2} \pm i\omega. \quad (4.26)$$

A general solution is given as

$$F_1(t) = F_0(t+T) - \delta + e^{-(a/2)t} (A \sin \omega t + B \cos \omega t). \quad (4.27)$$

The constants A and B are determined as $A = a\delta/\omega$ and $B = 0$, by the requirement that $F_0(t)$ and $F_1(t)$ must be continuous up to the first derivative at $t = 0$. Therefore,

$$F_1(t) = \frac{\delta}{1 - e^{-aT}} (1 - e^{-a(t+T)}) - \delta + \frac{a\delta}{\omega} e^{-(a/2)t} \sin \omega t, \quad (4.28)$$

and the headway and the velocity for the n th vehicle is given as

$$\Delta x_n(t) = F_0(t+T) - F_1(t) + v_B T = \Delta x_A - \frac{a\delta}{\omega} e^{-(a/2)t} \sin \omega t,$$

$$\dot{x}_n(t) = \dot{F}_1(t) = \frac{a\delta}{e^{aT} - 1} e^{-at}$$

$$+ \frac{a\delta}{\omega} e^{-(a/2)t} \left(\omega \cos \omega t - \frac{a}{2} \sin \omega t \right). \quad (4.29)$$

We would now like to give general formula for $F_k(t)$ (for $t \in I_k = [-kT, -(k-1)T]$) with $k > 1$. Suppose that $F_k(t)$ for $t \in I_k$ is known to us and we are trying to find $F_{k+1}(t)$ for $t \in I_{k+1}$. $F_{k+1}(t)$ satisfies the second order linear differential equation

$$\mathcal{D}F_{k+1}(t) = F_k(t+T) - \delta, \quad (4.30)$$

with boundary conditions

$$\begin{aligned} F_{k+1}(-kT) &= F_k(-kT), \\ \dot{F}_{k+1}(-kT) &= \dot{F}_k(-kT), \end{aligned} \quad (4.31)$$

while $F_k(t)$ satisfies a similar equation

$$\mathcal{D}F_k(t) = F_{k-1}(t+T) - \delta. \quad (4.32)$$

The function $F_k(t)$ describes the behavior of the n th vehicle only for $t \in I_k$. However we will find it useful to define the function by the relation (4.32) even outside the interval I_k . The function used outside the interval will be denoted as $\tilde{F}_k(t)$. The difference of Eqs. (4.30) and (4.32) gives us the following equation for $t \in I_{k+1} = [-(k+1)T, -kT]$:

$$\mathcal{D}(F_{k+1}(t) - \tilde{F}_k(t)) = F_k(t+T) - \tilde{F}_{k-1}(t+T) \quad (k \geq 1). \quad (4.33)$$

From Eqs. (4.24) and (4.25) we find

$$\mathcal{D}(F_1(t) - \tilde{F}_0(t)) = F_0(t+T) - \tilde{F}_0(t) - \delta = \delta(e^{-at} - 1), \quad (4.34)$$

for $t \in I_1 = [-T, 0]$.

By using the function $G_k(t)$ defined in the relation,

$$F_{k+1}(t) = \tilde{F}_k(t) + G_{k+1}(t+kT), \quad (4.35)$$

Eqs. (4.33) and (4.34) are rewritten into the following equations for $-T \leq t \leq 0$:

$$DG_{k+1}(t) = G_k(t) \quad (k \geq 1), \quad (4.36)$$

$$DG_1(t) = \delta(e^{-at} - 1) \equiv G_0(t). \quad (4.37)$$

Note that $G_0(t)$ defined in Eq. (4.37) satisfies $DG_0(t) = G_0(t)$. The conditions (4.31) become $G_k(0) = 0$ and $\dot{G}_k(0) = 0$ (for $k \geq 1$).

The Rondo function $F(t)$ for region II is given as a sum of $G_k(t)$,

$$F^{\text{II}}(t) = F_0(t) + \sum_{k \geq 0} \theta(-t - kT) G_{k+1}(t + kT), \quad (4.38)$$

for $t > -\tau$. In Appendix B we will give general solutions to differential equations (4.36) and (4.37). $G_1(t)$ from the appendix,

$$G_1(t) = G_0(t) + \frac{a\delta}{\omega} e^{-(a/2)t} \sin \omega t = \delta(e^{-at} - 1) + \frac{a\delta}{\omega} e^{-(a/2)t} \sin \omega t, \quad (4.39)$$

is consistent with Eq. (4.28). Similarly $G_2(t)$ is given as

$$G_2(t) = G_1(t) - \frac{a\delta}{\omega} \frac{2f}{4f-a} e^{-(a/2)t} \{ \omega t \cos \omega t - \sin \omega t \}. \quad (4.40)$$

So $F_2(t)$ for $t \in I_2 = [-2T, -T]$ becomes

$$\begin{aligned} F_2(t) &= \tilde{F}_1(t) + G_2(t+T) \\ &= \tilde{F}_1(t) + \delta(e^{-a(t+T)} - 1) \\ &\quad + \frac{a\delta}{\omega} e^{-(a/2)(t+T)} \sin \omega(t+T) \\ &\quad - \frac{a\delta}{\omega} \frac{2f}{4f-a} e^{-(a/2)(t+T)} \{ \omega(t+T) \cos \omega(t+T) \\ &\quad - \sin \omega(t+T) \}, \end{aligned} \quad (4.41)$$

while the headway for the n th vehicle is

$$\begin{aligned} \Delta x_n(t) &= \Delta x_A - \frac{a\delta}{\omega} e^{-(a/2)t} \sin \omega t + \frac{a\delta}{\omega} \frac{2f}{4f-a} e^{-(a/2)(t+T)} \\ &\quad \times \{ \omega(t+T) \cos \omega(t+T) - \sin \omega(t+T) \}. \end{aligned} \quad (4.42)$$

The general formula in Appendix B may be used further to generate F_3, F_4, \dots , needed to describe the trajectory in region II.

Let us consider region III. At $t = -\tau$, the function (4.38) for region II must be continuously connected to $F^{\text{III}}(t)$, including their first derivatives. This condition yields $F^{\text{III}}(t)$ for $t \leq -\tau$ as

$$F^{\text{III}}(t) = V_0(t + \tau) + F^{\text{II}}(-\tau). \quad (4.43)$$

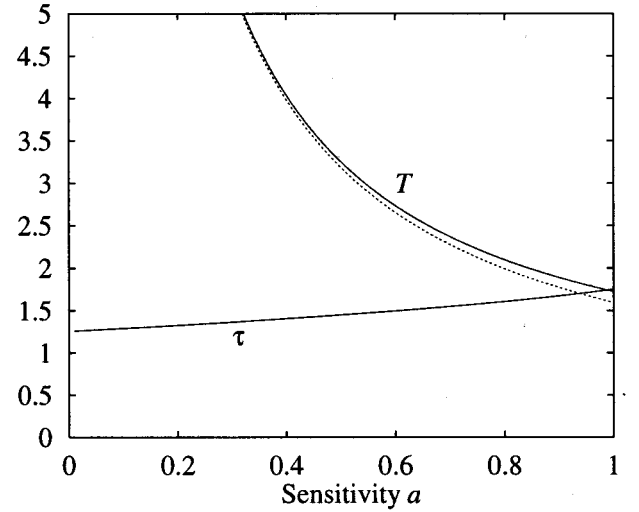


FIG. 5. Sensitivity dependence of T and τ for the single slope function model. The condition, $T \geq \tau$, is assumed, which is satisfied for $a \leq 0.98857 \dots$. The dotted line shows the a - T relation for the step function model.

The continuity condition for the first derivative requires also that

$$\dot{F}^{\text{II}}(-\tau) = \dot{F}^{\text{III}}(-\tau) \equiv V_0. \quad (4.44)$$

This completes our construction of an asymptotic trajectory.

Now let us find the a dependence of T for the present model. The time $-\tau$ may be determined by the condition (4.13), $F(-\tau + T) - F^{\text{II}}(-\tau) + v_B T = \Delta x_B$; then Eq. (4.44) gives us a relation between a and T . By using Eq. (4.38) for $F^{\text{II}}(-\tau)$, concrete expressions of Eqs. (4.13) and (4.44) may be obtained. For $-T \leq -\tau$, $F^{\text{II}}(-\tau)$ is simply given by $F_1(-\tau)$ and the above conditions are expressed as

$$\frac{a\delta}{\omega} e^{(a/2)\tau} \sin \omega \tau = \Delta x_B - \Delta x_A \equiv \frac{V_0}{f}, \quad (4.45)$$

$$\frac{a\delta}{e^{aT} - 1} e^{a\tau} + \frac{a\delta}{\omega} e^{(a/2)\tau} \left(\omega \cos \omega \tau + \frac{a}{2} \sin \omega \tau \right) = V_0. \quad (4.46)$$

The requirement of symmetry $\Delta x_n(+\infty) + \Delta x_n(-\infty) = 2\Delta x_S$, mentioned in Sec. III becomes $v_B T + (V_0 + v_B)T = 2\Delta x_S$. This relation and Eq. (4.10) allow us to express $\delta = \Delta x_A - v_B T$ as,

$$\delta = (fT - 1) \frac{V_0}{2f}. \quad (4.47)$$

Finally, we reach to the coupled equations which determine T and τ for a given slope f and sensitivity a

$$\begin{cases} (fT - 1) e^{(a/2)\tau} \sin \omega \tau = \frac{2\omega}{a}, \\ (e^{aT} - 1) \left[\left(f - \frac{a}{2} \right) \sin \omega \tau - \omega \cos \omega \tau \right] = \omega e^{(a/2)\tau}, \end{cases} \quad (4.48)$$

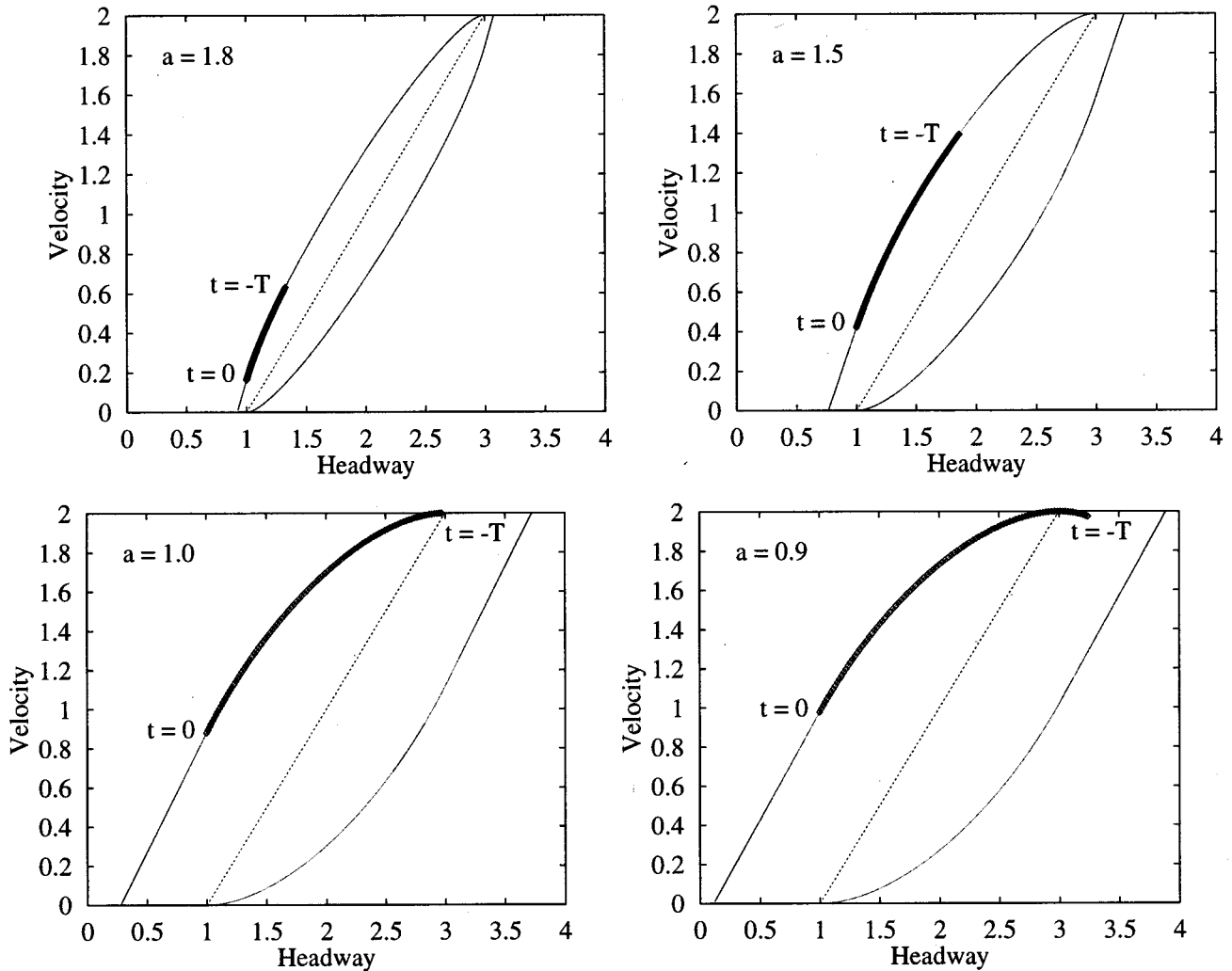


FIG. 6. Thin curves show “limit cycles” for the single slope function model obtained from simulations with (a) $a=1.8$, (b) $a=1.5$, (c) $a=1.0$, and (d) $a=0.9$. Trajectories generated from $F_1(t)$ for $t \in [-T, 0]$ are drawn with thick curves. The curves inside region II ($1 < \Delta x < 3$) are parts of asymptotic trajectories. The dotted line shows the OV function with $f=1.0$, $V_0=2.0$, and $\Delta x_s=2.0$.

where ω is given in Eq. (4.26). For $f=1.0$, Eq. (4.48) is solved numerically to give the a dependence of T and τ as shown in Fig. 5. Since we used $F_1(t)$ for $F^{II}(t)$, Eq. (4.48) is valid only for $\tau \leq T$ (τ coincides with T when $a=0.98857\dots$ at $\tau=T=1.74027\dots$).

We observe in Fig. 5 that T behaves as $1/a$ for small a : this implies that, for congested flows to be formed, the delay T must be larger for less sensitive drivers. In the limit of $f \rightarrow \infty$, the present model reduces to the step function model, in which $aT = \rho$ and $\tau = 0$. This may be confirmed with Eq. (4.48) since aT reaches a constant, $\rho = 1.59362\dots$, and $a\tau$ behaves like $2a/(f\rho)$ when a/f goes to zero (note that Eq. (4.48) may be rewritten in terms of rescaled variables aT , $a\tau$, and a/f).

In order to see the validity of our approach, let us compare our results and trajectories obtained by simulations. In Fig. 6, thick curves show parts of the asymptotic trajectories, to be determined by the function $F_1(t)$, for $a=1.8$, 1.5 ($\tau > T$), $a=1.0$ ($\tau \sim T$), and $a=0.9$ ($\tau < T$). These curves are to be compared with numerical simulations shown as thin

curves. The function $F_1(t)$ is enough to give an asymptotic trajectory for $a \leq 0.98857\dots$, as mentioned above. It is expected that when a gets closer to its critical value ($a_{\text{critical}} = 2f = 2.0$, in this case), we need functions $F_k(t)$ with a higher k to form an entire trajectory.

There again appears a flat trajectory in region III. As in the step function model, it takes time T for a vehicle to move on the flat trajectory and there is only one vehicle traveling on this interval.

C. Double slope function model

The OV function for the single slope model has flat regions I and III, like the step function model. For those regions the Rondo equation does not depend on $F(t+T)$: a vehicle does not react to the motion of the preceding one. This motivates us to consider a more realistic model with an OV function which has a nonzero gradient for any headway.

The OV function has a slope f_1 in regions I and III, and f_2 in region II (see Fig. 7)

$$V(\Delta x) = \begin{cases} f_1 \Delta x & \Delta x \leq \Delta x_A & \text{(region I)} \\ f_2 [\Delta x - (1 - \kappa) \Delta x_A] & \Delta x_A \leq \Delta x \leq \Delta x_B & \text{(region II)} \\ f_1 [\Delta x + (\kappa^{-1} - 1)(\Delta x_B - \Delta x_A)] & \Delta x_B \leq \Delta x & \text{(region III)}. \end{cases} \quad (4.49)$$

where $\kappa = f_1/f_2$. Obviously this function is symmetric around $(\Delta x_S, V(\Delta x_S))$, where Δx_S is the middle point of region II. Here we should note that the sensitivity a must satisfy $f_1 < a/2 < f_2$ for a generation of the congestion in this model, since the homogeneous flow is expected to be linearly unstable only in region II.

As in Sec. IV B, we assume that the headway reaches Δx_B at $t = -\tau$ and Δx_A at $t = 0$. The solution of the Rondo equation (3.4) must satisfy the conditions (4.12), (4.13). The Rondo function $F(t)$ for three regions will be denoted as follows;

$$F(t) = \begin{cases} F^I(t) & (0 \leq t) \\ F^{II}(t) & (-\tau \leq t \leq 0) \\ F^{III}(t) & (t \leq -\tau). \end{cases} \quad (4.50)$$

For $F^I(t)$ ($t \geq 0$), the Rondo equation is given by

$$\mathcal{D}_1 F^I(t) = F^I(t+T) + v_B T, \quad (4.51)$$

where

$$\mathcal{D}_1 = \frac{1}{af_1} \frac{d^2}{dt^2} + \frac{1}{f_1} \frac{d}{dt} + 1. \quad (4.52)$$

To find a solution to the homogeneous equation $\mathcal{D}_1 F_{\text{hom}}^I(t) = F_{\text{hom}}^I(t+T)$, we use the ansatz $F_{\text{hom}}^I(t) \sim e^{\gamma t}$ which gives an equation for the exponent γ ,

$$\frac{\gamma^2}{a} + \gamma = f_1 (e^{\gamma T} - 1). \quad (4.53)$$

As long as the condition $f_1 < 1/T$ holds (when a congested flow is realized in this model, this condition is satisfied trivially), there are two real solutions: the negative $-\gamma_{\text{in}}$ and the positive one γ_{out} . Because of the asymptotic behavior, $\dot{F}(t) \rightarrow v_C$ as $t \rightarrow +\infty$, only the exponent $-\gamma_{\text{in}}$ is relevant to the function $F^I(t)$. Adding a particular solution of Eq. (4.51), we obtain the solution subject to conditions (4.12) and $F(0) = 0$ as

$$F^I(t) = v_C t + (\Delta x_A - \Delta x_C) \frac{1 - e^{-\gamma_{\text{in}} t}}{1 - e^{-\gamma_{\text{in}} T}}. \quad (4.54)$$

By calculating $\Delta x_n(t)$ and $\dot{x}_n(t)$ from Eq. (4.54),

$$\Delta x_n(t) = \Delta x_C + (\Delta x_A - \Delta x_C) e^{-\gamma_{\text{in}} t}, \quad (4.55)$$

$$\dot{x}_n(t) = v_C + (\Delta x_A - \Delta x_C) \frac{\gamma_{\text{in}}}{1 - e^{-\gamma_{\text{in}} T}} e^{-\gamma_{\text{in}} t}, \quad (4.56)$$

we obtain a linear trajectory given by

$$\dot{x}_n(t) - v_C = \frac{\gamma_{\text{in}}}{1 - e^{-\gamma_{\text{in}} T}} [\Delta x_n(t) - \Delta x_C]. \quad (4.57)$$

In region II the function $F^{II}(t)$ is divided into $F_k(t)$'s for $t \in I_k = [-kT, -(k-1)T]$ as was done in Sec. IV B. We may now study the Rondo equation,

$$\mathcal{D}_2 F_k(t) = F_{k-1}(t+T) + v_B T - (1 - \kappa) \Delta x_A (k \geq 1), \quad (4.58)$$

where $F_0(t) \equiv F^I(t)$ and \mathcal{D}_2 is \mathcal{D}_1 with f_1 replaced by f_2 : $\mathcal{D}_2 = \mathcal{D}_1 - (1 - \kappa)(\mathcal{D}_1 - 1)$. In terms of \mathcal{D}_2 , Eq. (4.51) becomes

$$\mathcal{D}_2 F_0(t) = F_0(t+T) + v_B T - (1 - \kappa) \Delta x_n(t), \quad (4.59)$$

where $\Delta x_n(t)$ is given by Eq. (4.55).

The basic technique in Sec. IV B may be used to solve Eq. (4.58) with a slight modification. Let us define $G_k(t)$'s with $F_{k+1}(t) = \tilde{F}_k(t) + G_{k+1}(t+kT)$, which satisfy the equations

$$\mathcal{D}_2 G_{k+1}(t) = G_k(t) \quad (k \geq 1), \quad (4.60)$$

$$\mathcal{D}_2 G_1(t) = \delta (e^{-\gamma_{\text{in}} t} - 1) \equiv G_0(t), \quad (4.61)$$

where $\delta = (1 - \kappa)(\Delta x_A - \Delta x_C)$. The boundary conditions are $G_k(0) = \dot{G}_k(0) = 0$ for $k \geq 1$. In solving these, we may use again the formula given in Appendix B. Once we find the series of $G_k(t)$, we obtain the function $F^{II}(t)$ by the relation (4.38). Further we can determine the time $-\tau$ by the condition (4.13), $F(-\tau+T) - F^{II}(-\tau) + v_B T = \Delta x_B$.

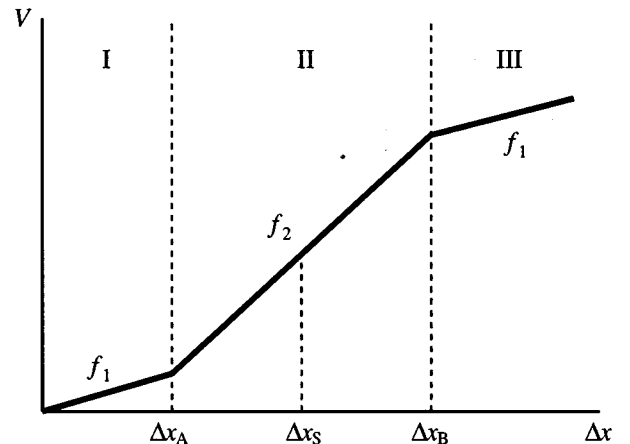


FIG. 7. The OV function for the double slope function model, which is symmetric with respect to the point $(\Delta x_S, V(\Delta x_S))$. It has the gradient $f_1(f_2)$ in regions I and III (II).

In region III ($t \leq -\tau$), the Rondo equation takes the form

$$D_1 F^{\text{III}}(t) = F^{\text{X}}(t+T) + v_B T + (\kappa^{-1} - 1)(\Delta x_B - \Delta x_A), \quad (4.62)$$

where $F^{\text{X}}(t+T)$ is $F^{\text{II}}(t+T)$ for $-\tau \leq t+T \leq -\tau+T$ and $F^{\text{III}}(t+T)$ for $t+T \leq -\tau$. The solution must be continuously connected to $F^{\text{II}}(t)$ including the first derivative at $t = -\tau$. Equation (4.62) can be solved by the same manner as in region II, though homogeneous solutions to Eq. (4.62) include the hyperbolic functions instead of the trigonometric functions.

The logic at the end of Sec. III may be used to get a better perspective on what we have discussed up to now, and it will lead us to find the a dependence of T . First, with a given slope T^{-1} , we draw a straight line through point S . The value of $-v_B$ and the coordinates of C and F are given in terms of T and the parameters in the OV function,

$$v_C = \frac{f_1 T}{1 - f_1 T} v_B, \quad \Delta x_C = \frac{v_B T}{1 - f_1 T}, \quad (4.63)$$

$$v_F = \frac{f_1 v_B T + f_1 (\kappa^{-1} - 1)(\Delta x_B - \Delta x_A)}{1 - f_1 T},$$

$$\Delta x_F = \frac{v_B T + f_1 T (\kappa^{-1} - 1)(\Delta x_B - \Delta x_A)}{1 - f_1 T}, \quad (4.64)$$

and

$$-v_B = \left(f_1 - \frac{f_2 T + 1}{2T} \right) \Delta x_A + \frac{f_2 T - 1}{2T} \Delta x_B. \quad (4.65)$$

In solving the Rondo equation, we have introduced a parameter τ determined by Eq. (4.13). Using this τ and v_B expressed as Eq. (4.65), we obtain a one-parameter family of the (a -dependent) solution to the Rondo equation. Then, we find an appropriate value of a for a given T by the requirement that the asymptotic trajectory connects C and F : $\dot{F}^{\text{III}}(-\infty) = v_F$.

In Fig. 8, we show trajectories from our analytic study and a computer simulation for the double slope model. We have chosen a particular value for a so that $\tau = T$ and we used the Rondo function for $t > -\tau - T$ to draw the part of the decelerating asymptotic trajectory. Clearly the Rondo function reproduces the trajectory obtained via a computer simulation.

By the procedure described in this subsection, we may easily obtain the remaining part of the asymptotic trajectory. When this is carried out, we expect that it reaches to point F in the infinite past. In the following we will give another argument to support this expectation. The Rondo equation for $t < -\tau - T$ in region III may be solved with exponential functions plus a particular solution, as for region I: the function $F^{\text{III}}(t)$ is the sum of a term linear in t and exponential functions. In the limit $t \rightarrow -\infty$, only the linear term survives expressing that vehicles have the velocity for a free region v_F ; the exponents satisfy Eq. (4.53) and have positive real parts so that exponential functions vanish as $t \rightarrow -\infty$.

It would be appropriate to explain how solutions to Eq. (4.53) are distributed on the complex γ plane. Without going

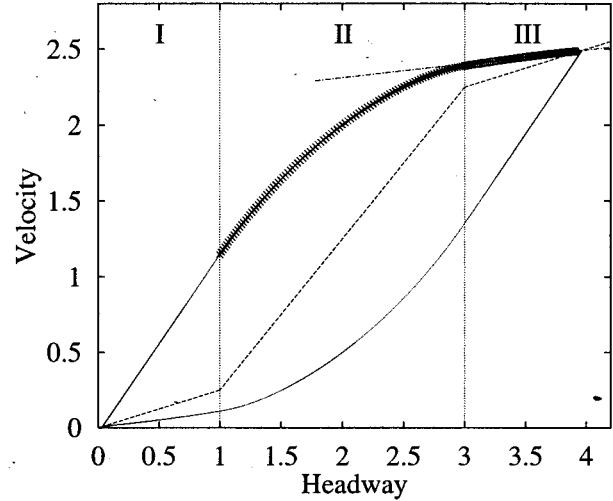


FIG. 8. Trajectories for the double slope model. Thin curve shows “limit cycle” from simulation with $a = 1.13124$ when $T = \tau = 1.58331$. The analytical solution is drawn with a thick curve. The dotted-dashed line shows the trajectory expressed by the exponential function with index γ_{out} . The dotted line shows the OV function with $f_1 = 0.25, f_2 = 1.0, \Delta x_A = 1.0$, and $\Delta x_B = 3.0$.

into the details, here we only quote features relevant to our arguments. There is only one solution with a negative real part, it is actually a real solution $-\gamma_{\text{in}}$. Other solutions have positive real parts, which are relevant when $t \sim -\infty$. There is only one real solution, γ_{out} ; there are complex pair solutions with their real parts larger than γ_{out} . Since γ_{out} has the smallest positive real part, it dominates among exponential functions when $t \rightarrow -\infty$. Thus for very large negative t , the function $F^{\text{III}}(t)$ may be approximated by the exponential functions with γ_{out} . In region I, we found that the decelerating asymptotic trajectory is linear on the Δx - v plane owing to the exponential term in $F^{\text{I}}(t)$. Similarly, the approximated $F^{\text{III}}(t)$ defines a line on the Δx - v plane, starting point F as shown in Fig. 8. We observe that this line is actually the tangent line to the trajectory at point F .

The absence of the flat region is directly related to our observation that point F is reached only in the infinite past. If we consider the limit to have a flat region $f_1 = 0$, we only have a negative solution $\gamma_{\text{in}} = -a$. When we would like to consider the OV model applied for a realistic situation, the relevant OV function may be approximately realized by a piecewise linear function. Since it is unlikely that the function has a flat region, the above feature of the double slope model must be generic.

V. TRAJECTORIES AROUND CUSPS

In Sec. IV, we discussed asymptotic trajectories in models with piecewise linear OV functions. The asymptotic trajectories can be realized only when the number of vehicles becomes infinite. In computer simulations in Refs. [1–3], a finite number of vehicles run around a circuit; a vehicle goes through all the free and congested regions in a finite time. The Rondo equation probably has solutions even for such situations. Though we have not worked out how to obtain entire trajectories for such vehicles, we are able to discuss

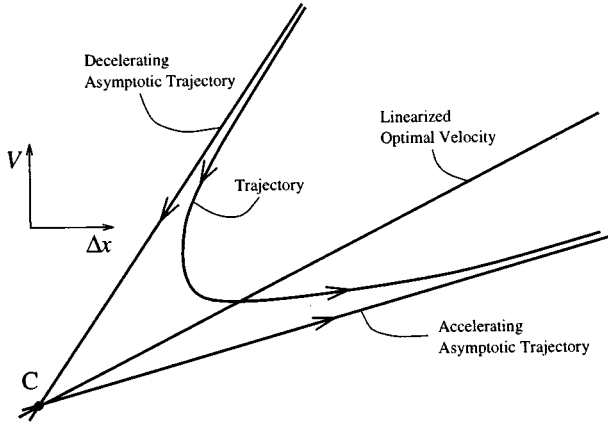


FIG. 9. A trajectory in linear approximation for a vehicle passing through the congested region with a finite size. It has two asymptotes, accelerating and decelerating asymptotic trajectories. The time development is indicated with arrows.

parts of the trajectories around points C or F . We are going to discuss this subject in this section.

To make our explanation concrete, we take a trajectory around the end point C . In a congested region, all the vehicles have almost the same velocity. When a vehicle is about to reach a congested region, its velocity would be slightly different from v_C and the function $F(t)$ may be written as $F(t) = v_C t + \xi(t)$. We take a linear approximation for an OV function $V(\Delta x)$ (here as an OV function we have in mind a smooth, but not necessarily a piecewise linear, function) around the point $(\Delta x_C, v_C)$,

$$V(\Delta x) \approx f_C(\Delta x - \Delta x_C) + v_C. \quad (5.1)$$

Since $(v_B + v_C)T = \Delta x_C$, the Rondo equation (3.4) becomes a linear difference-differential equation for $\xi(t)$,

$$\frac{\ddot{\xi}(t)}{a} + \dot{\xi}(t) = f_C[\xi(t+T) - \xi(t)]. \quad (5.2)$$

For the ansatz $\xi(t) = e^{\gamma t}$, we find an equation for the exponent γ ,

$$\frac{\gamma^2}{a} + \gamma = f_C(e^{\gamma T} - 1). \quad (5.3)$$

As long as $f_C < 1/T$, there are two real solutions: the negative, $-\gamma_{in}$, and the positive one, γ_{out} (we ignored complex solutions in this approximation since the real part of those solutions is larger than γ_{out} . See the discussion in Sec. VI).

Trajectories considered here cross (at $t=0$) the OV function at points slightly different from C : we denote their coordinates by $(\Delta x, v) = (\Delta x_C + \delta v/f_C, v_C + \delta v)$. We find the solution for $F(t)$ as,

$$F(t) = v_C t + \frac{-\gamma_{out}^2 e^{-\gamma_{in} t} + \gamma_{in}^2 e^{\gamma_{out} t}}{\gamma_{in} \gamma_{out} (\gamma_{in} + \gamma_{out})} \delta v. \quad (5.4)$$

We may find $\Delta x_n(t)$ and $v_n(t)$ from this solution

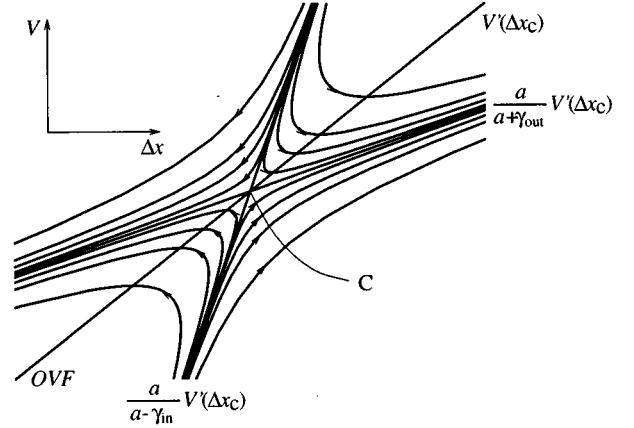


FIG. 10. The flow diagram around point C obtained by the linear approximation. Two asymptotes are asymptotic trajectories.

$$\Delta x_n(t) = \Delta x_C + \frac{(a - \gamma_{in}) \gamma_{out} e^{-\gamma_{in} t} + (a + \gamma_{out}) \gamma_{in} e^{\gamma_{out} t}}{a(\gamma_{in} + \gamma_{out})} \frac{\delta v}{f_C}, \quad (5.5)$$

$$v_n(t) = v_C + \frac{\gamma_{out} e^{-\gamma_{in} t} + \gamma_{in} e^{\gamma_{out} t}}{\gamma_{in} + \gamma_{out}} \delta v. \quad (5.6)$$

By eliminating the time t , we find the equation for the trajectory around point C

$$\left[\frac{af_C(\Delta x - \Delta x_C) - (a - \gamma_{in})(v - v_C)}{\gamma_{in} \delta v} \right]^{\gamma_{in}} \times \left[\frac{(a + \gamma_{out})(v - v_C) - af_C(\Delta x - \Delta x_C)}{\gamma_{out} \delta v} \right]^{\gamma_{out}} = 1. \quad (5.7)$$

This curve, shown in Fig. 9, has two asymptotes through C with slopes $af_C/(a - \gamma_{in})$ and $af_C/(a + \gamma_{out})$, which correspond to the decelerating and accelerating asymptotic trajectories, respectively.

Two asymptotes of Eq. (5.7) divide the Δx - v plane into four areas. In Fig. 10, curves are shown for solutions to Eq. (5.2) with various initial conditions: point C is a saddle point. The linear analysis applies to point F as well, so curves in the left-lower region would describe the behavior of vehicles close to a free region.

The condition, $[v(t) - v_C]/v_C \ll 1$, helps us to evaluate t_C , the time interval a vehicle would spend around point C ;

$$t^2 \ll \frac{2}{\gamma_{in} \gamma_{out}} \frac{v_C}{\delta v} \sim t_C^2. \quad (5.8)$$

The time t_C is related to the length of a congested region L_C and the number of vehicles in this region N_C as follows:

$$N_C = \frac{t_C}{T}, \quad L_C = N_C \Delta x_C = \Delta x_C \frac{t_C}{T}. \quad (5.9)$$

Therefore the size of a congested region is larger for smaller δv .

VI. SUMMARY AND DISCUSSION

We have investigated the repetitive pattern formation observed in a computer simulation from an analytical point of view. The Rondo approach was proposed to describe the repetitive pattern. In addition to a and $V(\Delta x)$, the difference-differential equation for the Rondo function $F(t)$ contains two macroscopic parameters, T and v_B , which specify the motion of a global pattern. In this paper we mainly paid attention to the Rondo functions for asymptotic trajectories. The Rondo equation was solved for three simple models with piecewise linear OV functions. In order to determine the a dependence of T and v_B , we gave analytic expressions for Rondo functions. We would like to emphasize that the concept of asymptotic trajectory plays a key role in determining the a dependence of T and v_B . As a first step to understand more realistic situations, we have studied some trajectories around cusps.

Our asymptotic trajectories were compared with closed trajectories obtained via simulations. Except for some details around cusps, the agreement is quite good. Our work is not the first one where the comparison was made between simulations and analytic results. In Ref. [14], Nagatani proposed a stochastic cellular automaton model for which the closed trajectory was analytically obtained with a mean field method. The analytic result recovers the simulations qualitatively for a certain range of acceleration in his model.

In the following we discuss four questions related to the Rondo approach: (1) a description of a homogeneous flow; (2) an extension to OV models with asymmetric OV functions; (3) more on realistic trajectories; and (4) a possibility to find the Rondo function *forward* in time.

It would be appropriate to mention how a homogeneous flow may be described in the Rondo approach. A homogeneous flow is described by the solution to the Rondo equation, $\dot{F}(t) = v_0 = \text{const}$, where T and v_B are chosen to satisfy the relation, $v_0 = V[(v_0 + v_B)T]$. The trajectory of the flow is represented by a single point on the OV function. We know that the instability of this trajectory to a small perturbation gives us a congested flow. The stability analysis of an asymptotic trajectory might help us to understand the nature of this pattern formation.

Studying more realistic models, we may encounter an asymmetric OV function. We explain how our procedure, developed in this paper, may be extended to such situations. Even with an asymmetric OV function, we may define the concept of accelerating and decelerating asymptotic trajectories. When the symmetry is absent, accelerating and decelerating asymptotic trajectories are not related to each other and must be found independently. The condition that both of them share the same end points C and F will determine the a dependence of T .

Even though we have mainly studied asymptotic trajectories, the Rondo equation itself must be applicable for any repetitive motion of vehicles. On the other hand, as we have observed for piecewise linear models, the difference between asymptotic trajectories and the results of computer simulations are very small. Therefore, whether we would like to obtain a realistic trajectory out of the Rondo approach or not very much depends on our purpose.

The Rondo equation gives us a functional relation which may be written as,

$$F(t+T) = \mathcal{P}[F(t), \dot{F}(t), \ddot{F}(t); a, v_B, T], \quad (6.1)$$

with three parameters a , v_B , and T . When we know the function $F(t)$ for the time interval $t \in [t_0, t_0 + T]$, there are two ways to use the above equation: (1) substituting this on the right-hand side, we find $F(t)$ for $t \in [t_0 + T, t_0 + 2T]$; (2) the same information may be used on the left-hand side to have a differential equation for $F(t)$ on the interval $t \in [t_0 - T, t_0]$. Although the former sounds much easier, we have been able to use the Rondo equation only in the latter manner. Here we will explain why.

Now let us consider, for concrete, a decelerating asymptotic trajectory in the double slope model. In order to use Eq. (6.1) in approach (1), we need the Rondo function describing a part of the asymptotic trajectory coming out of F ; the rest of the asymptotic trajectory may be obtained just by differentiating the initial function repeatedly. So the initial Rondo function is of vital importance.

Since the OV function is symmetric, the transcendental equation (4.53) may be used to find the initial Rondo function. Let us remember how solutions are distributed. There are only two real solutions, $-\gamma_{\text{in}} < 0$ and $\gamma_{\text{out}} > 0$, and infinitely many complex solutions whose real parts are larger than γ_{out} . The initial Rondo function is a linear combination of infinitely many exponential functions with $\text{Re}(\gamma) > 0$. Therefore, it contains infinitely many coefficients, which must be determined to give an asymptotic trajectory with properties described in Sec. III. To find an asymptotic trajectory in this way, we probably need some new techniques.

In this paper we have considered the repetitive pattern in traffic flow. Such a repetitive structure is also observed in various phenomena, and we believe that our approach may be helpful to understand them.

APPENDIX A: ASYMPTOTIC TRAJECTORY IS SYMMETRIC

In this paper we have used the following property of an asymptotic trajectory: $(\Delta x_C, v_C)$ and $(\Delta x_F, v_F)$ are at symmetric positions for OV function symmetric around a point S . Here we would like to give a proof of the above claim for an OV function symmetric with respect to the point S .

Suppose an OV-function function and a sensitivity are given. Our Rondo equation contains two parameters T and v_B

$$\frac{1}{a} \ddot{F}(t) + \dot{F}(t) = V[F(t+T) - F(t) + v_B T]. \quad (A1)$$

If we could find a solution $F(t)$ for the equation, this means that, for the OV function and the sensitivity a , a corresponding pattern with the delay T and the backward velocity v_B may be realized.

The OV function is taken to be an odd function around the point $S(\Delta x_S, v_S)$. This assumption is expressed with an odd function $W(-x) = -W(x)$ as follows:

$$V(\Delta x) = v_S + W(\Delta x - \Delta x_S). \quad (A2)$$

By putting this form to the Rondo equation, it now looks like,

$$\frac{1}{a}\ddot{F}(t) + \dot{F}(t) = v_S + W[F(t+T) - F(t) + v_B T - \Delta x_S]. \quad (\text{A3})$$

We assume that a solution to the Rondo equation has been found. It gives a trajectory on the Δx - v plane, whose coordinate we denote as $(\Delta x_1(t), v_1(t))$. They are expressed with the function $F(t)$ as follows:

$$v_1(t) = \dot{F}(t), \quad \Delta x_1(t) = F(t+T) - F(t) + v_B T. \quad (\text{A4})$$

By using the fact that W is odd, it is easily shown that $(\Delta x_2(t), v_2(t))$, given below, satisfies the Rondo equation as well.

$$v_2(t) = \dot{\bar{F}}(t), \quad \Delta x_2(t) = \bar{F}(t+T) - \bar{F}(t) + v'_B T, \quad (\text{A5})$$

where $\bar{F}(t) \equiv 2v_S t - F(t)$ and $v'_B T \equiv -2v_S T - v_B T + 2\Delta x_S$.

It is also easy to see that $(\Delta x_1(t), v_1(t))$ and $(\Delta x_2(t), v_2(t))$ are symmetric with respect to point S . Therefore, if the former defines a trajectory from a free to a congested region, the latter defines that for the opposite direction.

Here we emphasize that two trajectories have different backward velocities but with the same delay time T . In computer simulations, we observe that a pattern of a congested flow is characterized with two parameters T and v_B ; both regions, connecting free to congested or congested to free, move with the same backward velocity v_B . So two trajectories connecting free and congested regions must have the same parameters. This must be also true for an asymptotic trajectory. Therefore v'_B must be equal to v_B itself. This implies that the two trajectories discussed above form a closed trajectory. Thus we may conclude the following: (1) solutions expressed by $F(t)$ and $\bar{F}(t)$ satisfy the Rondo equation with the same parameters T and v_B ; (2) the two points on the OV function connected by trajectories are symmetric with respect to point S ; and (3) the straight line through the two points includes the point S .

APPENDIX B: GENERAL FORMULA FOR STEP-BY-STEP METHOD

In the following we will give a general formula for the second order linear differential equation:

$$\left(\frac{1}{af} \frac{d^2}{dt^2} + \frac{1}{f} \frac{d}{dt} + 1 \right) G_k(t) = G_{k-1}(t) \quad (\text{B1})$$

$$G_k(0) = 0, \quad \dot{G}_k(0) = 0 \quad (k \geq 1),$$

$$\left(\frac{1}{af} \frac{d^2}{dt^2} + \frac{1}{f} \frac{d}{dt} + 1 \right) G_0(t) = G_0(t) \quad (\text{B2})$$

$$G_0(0) = 0, \quad \dot{G}_0(0) = -a\delta.$$

The solution for Eq. (B2) is

$$G_0(t) = \delta(e^{-at} - 1). \quad (\text{B3})$$

In terms of the function $g_k(\theta)$ defined as follows:

$$G_{k+1}(t) = G_k(t) + \frac{a\delta}{\omega} \left(\frac{af}{\omega^2} \right)^k e^{-(a/2)t} g_k(\omega t) \quad (k \geq 0), \quad (\text{B4})$$

the initial conditions at $t=0$ are expressed as

$$g_k(0) = 0, \quad g'_k(0) = 0, \quad (k \geq 1) \quad (\text{B5})$$

$$g_0(0) = 0, \quad g'_0(0) = 1.$$

From Eqs. (B1), (B2), and $\omega^2 = af - a^2/4$, the equation to determine $g_k(\theta)$ is

$$g''_k(\theta) + g_k(\theta) = g_{k-1}(\theta) \quad (k \geq 1) \quad (\text{B6})$$

$$g''_0(\theta) + g_0(\theta) = 0.$$

The initial value problem with Eqs. (B5) and (B6) may be solved with the spherical Bessel functions $j_k(\theta)$ as

$$g_k(\theta) = \frac{1}{2^k k!} \theta^{k+1} j_k(\theta). \quad (\text{B7})$$

We give functions for $k=0, 1, 2, 3$ explicitly.

$$g_0(\theta) = \sin\theta,$$

$$g_1(\theta) = \frac{1}{2}(\sin\theta - \theta\cos\theta),$$

$$g_2(\theta) = \frac{1}{8}(3\sin\theta - 3\theta\cos\theta - \theta^2\sin\theta),$$

$$g_3(\theta) = \frac{1}{48}(15\sin\theta - 15\theta\cos\theta - 6\theta^2\sin\theta + \theta^3\cos\theta). \quad (\text{B8})$$

In this paper, we also use another series of solutions $h_k(t)$ of Eqs. (B6) with the initial condition

$$h_k(0) = 0, \quad h'_k(0) = 0, \quad (k \geq 1) \quad (\text{B9})$$

$$h_0(0) = 1, \quad h'_0(0) = 0.$$

It is easily shown that $h_k(\theta)$ is given by

$$h_k(\theta) = g'_k(\theta) \equiv \frac{\theta}{2k} g_{k-1}(\theta), \quad (\text{B10})$$

where the second equality is valid only for $k \geq 1$. We also give $h_k(\theta)$ for $k=0, 1, 2, 3$ explicitly.

$$h_0(\theta) = \cos\theta,$$

$$h_1(\theta) = \frac{1}{2}\theta\sin\theta,$$

$$h_2(\theta) = \frac{1}{8}(\theta\sin\theta - \theta^2\cos\theta),$$

$$h_3(\theta) = \frac{1}{48}(3\theta\sin\theta - 3\theta^2\cos\theta - \theta^3\sin\theta). \quad (\text{B11})$$

- [1] M. Bando, K. Hasebe, A. Nakayama, A. Shibata, and Y. Sugiyama, *Phys. Rev. E* **51**, 1035 (1995).
- [2] M. Bando, K. Hasebe, A. Nakayama, A. Shibata, and Y. Sugiyama, *Jpn. J. Ind. Appl. Math.* **11**, 203 (1994).
- [3] M. Bando, K. Hasebe, K. Nakanishi, A. Nakayama, A. Shibata, and Y. Sugiyama, *J. Phys. (France) I* **5**, 1389 (1995).
- [4] L. A. Pipes, *J. Appl. Phys.* **24**, 274 (1953).
- [5] G. F. Newell, *J. Oper. Res. Soc. Am.* **9**, 209 (1961).
- [6] D. C. Gazis, R. Herman, and R. W. Rothery, *J. Oper. Res. Soc. Am.* **9**, 545 (1961).
- [7] O. Biham, A. A. Middleton, and D. Levine, *Phys. Rev. A* **46**, 6124 (1992).
- [8] K. Nagel and M. Schreckenberg, *J. Phys. (France) I* **2**, 2221 (1992).
- [9] T. Nagatani, *J. Phys. Soc. Jpn.* **62**, 3837 (1993).
- [10] S. Yukawa, M. Kikuchi, and S. Tadaki, *J. Phys. Soc. Jpn.* **63**, 3609 (1994); S. Yukawa and M. Kikuchi, *ibid.* **64**, 35 (1995).
- [11] B. S. Kerner and P. Konhäuser, *Phys. Rev. E* **48**, 2335 (1993).
- [12] T. S. Komatsu and S. Sasa, *Phys. Rev. E* **52**, 5574 (1995).
- [13] Y. Sugiyama and H. Yamada, *Phys. Rev. E* **55**, 7749 (1997).
- [14] T. Nagatani, *Physica A* **223**, 137 (1996).